RSC Advances

Facile and large-scale synthesis of poly(m-phenylenediamine) nanobelts with high surface area and superior dye adsorption ability

Journal:	*RSC Advances*
Manuscript ID:	RA-ART-07-2014-006553.R1
Article Type:	Paper
Date Submitted by the Author:	07-Sep-2014

Complete List of Authors:	Meng, Yun; Central South University, Department of Environmental Engineering Zhang, Liyuan; Central South University, Department of Environmental Engineering Chai, Liyuan; Central South University, Department of Environmental Engineering Yu, Wanting; Central South University, Department of Environmental Engineering Wang, Ting; Central South University, Department of Environmental Engineering Dai, Shuo; Central South University, Department of Environmental Engineering Wang, Haiying; Central South University, Department of Environmental Engineering

The colour graphic:

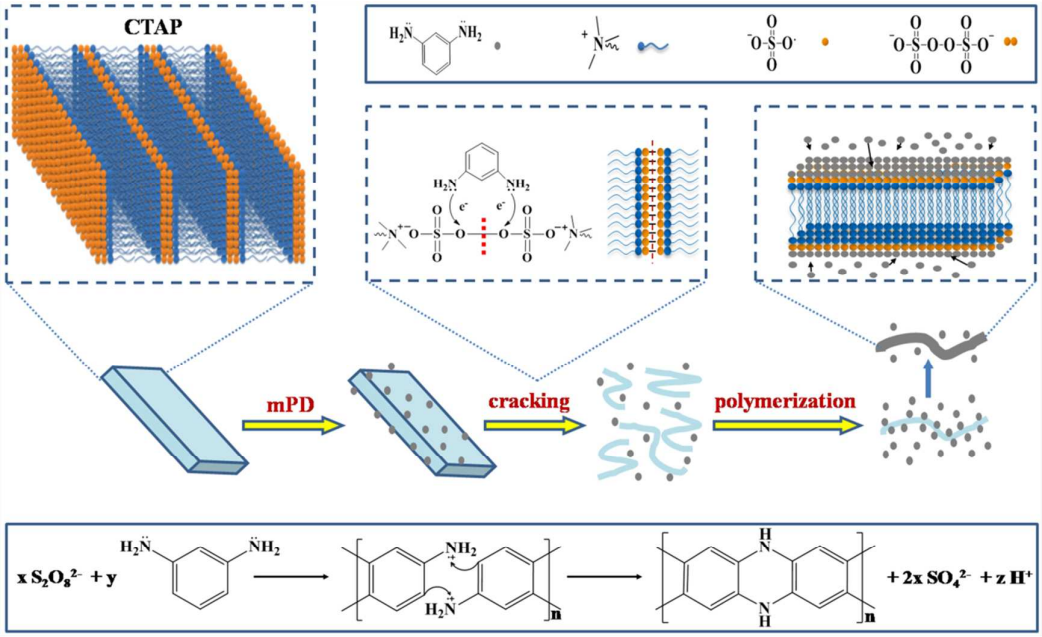

The text:

PmPD nanobelts with high adsorption performance have been synthesized by using CTAP as oxidants.

Cite this: DOI: 10.1039/c0xx00000x

www.rsc.org/advances

FULL PAPER

Facile and large-scale synthesis of poly(m-phenylenediamine) nanobelts with high surface area and superior dye adsorption ability

Yun Meng,[‡,a] Liyuan Zhang,[‡,a] Liyuan Chai,[a,b] Wanting Yu,[c] Ting Wang,[a] Shuo Dai[a] and Haiying Wang*[a,b]

Received (in XXX, XXX) Xth XXXXXXXXX 20XX, Accepted Xth XXXXXXXXX 20XX
DOI: 10.1039/b000000x

Uniform poly(m-phenylenediamine) (PmPD) nanobelts have been synthesized through chemical oxidative polymerization of m-phenylenediamine by using white cetyl trimethyl ammonium persulfate (CTAP) powders as oxidants. Results from Brunauer-Emmett-Teller (BET) method indicated that the surface area of PmPD reached as high as 284.5 $m^2 g^{-1}$. The function of high surface area on Orange G adsorption was examined. The Orange G adsorbance of PmPD can reach 469.5mg g^{-1}. The adsorption process can be better described by Langmuir and pseudo-second-order kinetic model. The acid doping of PmPD nanobelts could produce better adsorption performance for Orange G The superior performance of PmPD nanobelts endows them as hopeful functional materials for dye removal.

1. Introduction

Polyaniline is one of the most popular conjugated polymers (CPs) and has received tremendous amounts of attention in this decade. As a diamine derivative of polyaniline, poly(m-phenylenediamine) (PmPD) possesses multifunctionality and gradually becomes an important member in the family of CPs.[1] PmPD displays exceptional prospect in many applications,[2-5] typically water purification.[6-7] Li, Sun and our group have investigated the PmPD in removing heavy metal ions (e.g., Pb^{2+}, Ag^{+}, Hg^{2+}), dyes and anions [e.g., Cr(VI), SO_4^{2+}].[8-17] Its performance is superior as compared to the common adsorbents. For instance, the adsorbance (mg g^{-1}) of PmPD toward Ag^{+}, Cr(VI), Orange G can reach as high as ~2300, ~500, ~378 mg g^{-1}, respectively.

Recent development of nanoscience triggered increasing attention on size and morphology controllable synthesis of materials, since these two factors significantly affected materials' properties and performance.[18] To date, materials in nanoscale size with various shapes have been reported and nanobelts were particularly interesting.[19] Many efforts have been given to the synthesis of metal oxides nanobelts.[19] Limited examples have reported the fabrication of CPs nanobelts while the study of their applications was nearly missing. Moreover, seldom researches have successfully obtained the PmPD nanobelts.

In present research, we reported a facile fabrication of curved PmPD nanobelts, for the first time, by chemical oxidative polymerization using CTAP as oxidant. The PmPD nanobelts were characterized by Fourier transform infrared spectroscopy (FTIR), scanning electron microscope (SEM), transmission electron microscopy (TEM), N_2 adsorption-desorption isotherm and thermo gravimetric analyzer - differential thermal analysis (TGA-DTA). The adsorption performance of PmPD nanobelts toward Orange G and the effect of acid doping on the adsorptive property were investigated.

2. Experimental Section

2.1. Materials

The chemicals were of analytical grade. Cetyl trimethyl ammonium bromide (CTAB), sodium persulfate, and Orange G (OG) were purchased from Sinopharm Chemical (Shanghai, China), while the m-phenylenediamine (mPD) was from Acros (Belgium). Organic solvents, such as N-methyl-2-pyrrolidone (NMP), dimethyl sulfoxide (DMSO), N, N-Dimethylformamide (DMF), tetrahydrofuran (THF) and ethanol were from Hui-Hong Chemical (Hunan, China). Without special caution, de-ionized water was used throughout all experiments.

2.2. Polymerization procedures

In a typical experiment (Fig. S1, ESI†), 4.4 g sodium persulfate and m g CTAB (m = 1.69 g, 3.37 g, 6.74 g, 10.11 g) were dissolved in 50 mL de-ionized water respectively. The mixture was vigorously stirred for 20 min. Then 2.0 g mPD in 50 mL de-ionized water was rapidly poured into the mixture. The polymerization occurred as soon as the addition of mPD solution with stirring. The product was collected by vacuum filtration after 1 h, and rinsed with de-ionized water and ethanol at room temperature respectively. All products were dried at 60 °C under vacuum for 12 h. The sample was named PmPD-CTAP(x), where the x represents the molar ratio of CTAP to mPD. In addition, the poly(m-phenylenediamine) samples which were acid-doped with 1 M HCl solution have been named PmPD-CTAP (x)-P, where the P means protonation (acid doping).

2.3. Characterization

The morphologies of the samples were characterized by SEM (JSM-6360) and TEM (TECNAI G^2), with accelerating voltages of 20 kV and 120 kV, respectively. The supermolecular structure was determined by XRD (Scintag XDS 2000 powder diffractometer) at 45 kV and 40 mA from 5° to 80° with a Ni-filtered Cu KR1 radiation (λ) 1.542 Å). FTIR spectra were acquired in the range of 4000-1000 cm^{-1} at 32 scans with resolution of 4 cm^{-1} through Nicolet IS10 spectrometer. The thermal behaviors were recorded by heating in N_2 atmosphere at 10 °C min^{-1} from 30 to 800 °C with a TGA-50, Shimadzu. The surface area, pore volume, and pore size distribution of the polymer samples were determined from N_2 adsorption-desorption isotherms at 77 K by the BET equation in a relative pressure range of P/P_0 0.06-1 and the Barrett-Joyner-Halenda (BJH) method from the adsorption branch of the isotherms using ASAP 2050 analyzer (Micromeritics).

2.4. Adsorption method

Experiments were performed by consulting the research of Patil and Ayad[20-21], the calibration curve was in accordance with our previous researches[22]. All batch experiments were placed on a shaker at 120 rpm under controlled temperature of 30±1 °C. The concentration of Orange G was carefully analyzed using the U-4100 at the maximum absorbance of 480 nm[21]. The adsorbents used in the experiments include poly(m-phenylenediamine) and acid-doped poly(m-phenylenediamine).

Isotherm The adsorption isotherm was studied by adjusting the concentration of Orange G solution from 50 mg L^{-1} to 1500 mg L^{-1}, selecting 25 mg adsorbents and 20 mL Orange G solution, and shaking for 24 h . Langmuir and Freundlich models (Eq. 1, 2) were applied to study the isotherm adsorption of the PmPD.

$$Q = \frac{(C_0 - C_e)}{M} \cdot V \quad (1)$$

$$\frac{C_e}{Q_e} = \frac{C_e}{Q_m} + \frac{1}{K_a Q_m} \quad (2)$$

$$\log Q_e = \frac{1}{n} \log C_e + \log K_f \quad (3)$$

where C_0 is the initial concentration of the Orange G, C_e is the equilibrium concentration of the dye solution, V is the volume of the solution and the M is the mass of PmPD taken for the experiment. Q (mg g^{-1}) is the Orange G adsorbance of the PmPD, Q_e (mg g^{-1}) is the equilibrium Orange G adsorbance of the PmPD. Q_m (mg g^{-1}) is the maximum adsorption capacity, K_a (L mg^{-1}) is the adsorption coefficient, K_f and n are the equilibrium constants.

Kinetics The adsorption kinetics experiments were carried out in Teflon bottles, containing 20 mL of Orange G solution with the initial concentration of 400 mg L^{-1}, and 20 mg amount of adsorbents, then the mixture was shaken in different time intervals, the range of PmPD-CTAP (x) samples were from 10 to 1200 min, and the range of PmPD-CTAP (x)-P samples were from 10 to 180 min. Two kinetic models were tested in order to predict the adsorption data of Orange G as function of time using pseudo-first-order and pseudo-second-order kinetic models.

$$\log(Q_e - Q_t) = \log Q_e' - \frac{k}{2.303} t \quad (4)$$

$$\frac{t}{Q_t} = \frac{1}{h Q_e'^2} + \frac{t}{Q_e'} \quad (5)$$

where Q_e and Q_e' (mg g^{-1}) are the equilibrium and calculated Orange G adsorbance of the PmPD, Q_t (mg g^{-1}) is the Orange G adsorbance of the PmPD at specific time (t, min), k and h are the rate constants of first and second order equations, respectively.

3. Results and Discussion

3.1. Synthesis and morphology of poly(m-phenylenediamine)

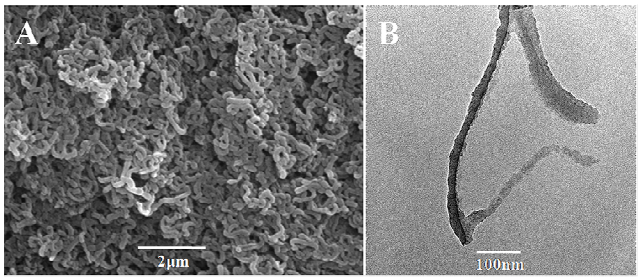

Fig.1 SEM (A) and TEM (B) images of poly(m-phenylenediamine) nanobelts by the CTAP : mPD molar ratio of 0.25:1.

The introduction of sodium persulfate into the CTAB solution immediately caused the formation of white CTAP powders (Fig.S2, ESI†), which was formed by the static interaction of two CTAB molecules with one persulfate anion.[23] When pouring m-phenylenediamine solution into the CTAP-containing solution, oxidative polymerization was initiated rapidly to generate black polymer powders. Fig. 1 provided the SEM and TEM images of poly(m-phenylenediamine) with CTAP : monomer molar ratio of 0.25 : 1. As seen, the polymer displays fibrous morphology, which is uniform and interconnected with each other (Fig.1A, SEM). From TEM in Fig.1B, the fibers are actually the flat belts and the width is in the range of 80-120 nm while the length is obviously more than 5 μm, indicating a high aspect ratio of the poly(m-phenylenediamine) nanobelts.

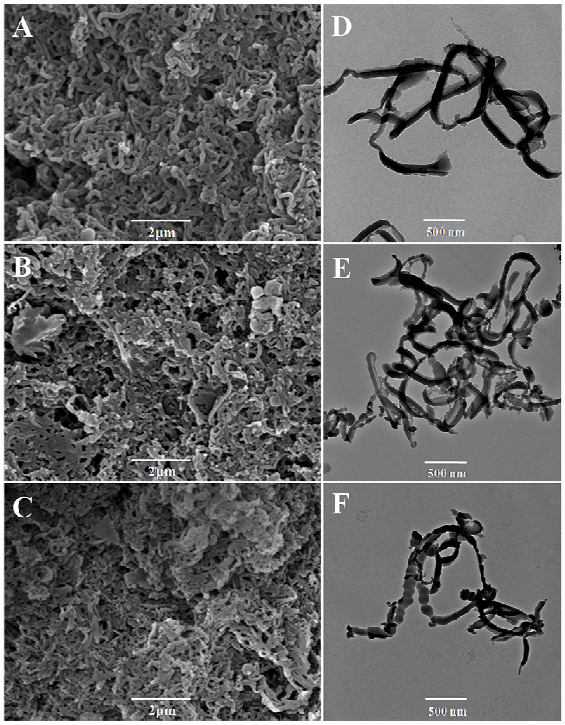

Fig.2 SEM and TEM images of poly(m-phenylenediamine) nanobelts synthesized with CTAP : mPD molar ratio of 0.125 (A, D), 0.5 (B, E), 0.75 (C, F).

In previous researches, organic solvents were used to mediate the morphology evolution of poly(m-phenylenediamine) to produce one dimension microstructures.[4, 13] However, primarily the rod-like morphology was obtained (Fig.S3, ESI†). As far as we are concerned, this may be the first example synthesizing the poly(m-phenylene-diamine) nanobelts. On the other hand, the intrinsic morphology of poly(m-phenylenediamine) is sphere when prepared in aqueous medium with traditional oxidation polymerization, according to the our previous researches (Fig.S4, ESI†).[6] That is to say, the use of CTAP as oxidants apparently alters the morphology evolution process of poly(m-phenylenediamine).

Moreover, the dosage of CTAP on the morphology of poly(m-phenylenediamine) was also investigated. As shown in Fig. 2, when increasing the CTAP: monomer ratio (A, B, C), the polymer belts became thinner; while increasing the CTAP ratio (Fig. 2D, E, F), the diameter of the belts obviously decreased and spherical morphology gradually emerged. In other words, increasing the monomer ratio to CTAP is not beneficial to acquire the uniform poly(m-phenylenediamine) nanobelts.

Scheme 1. Possible morphology evolution of PmPD nanobelts

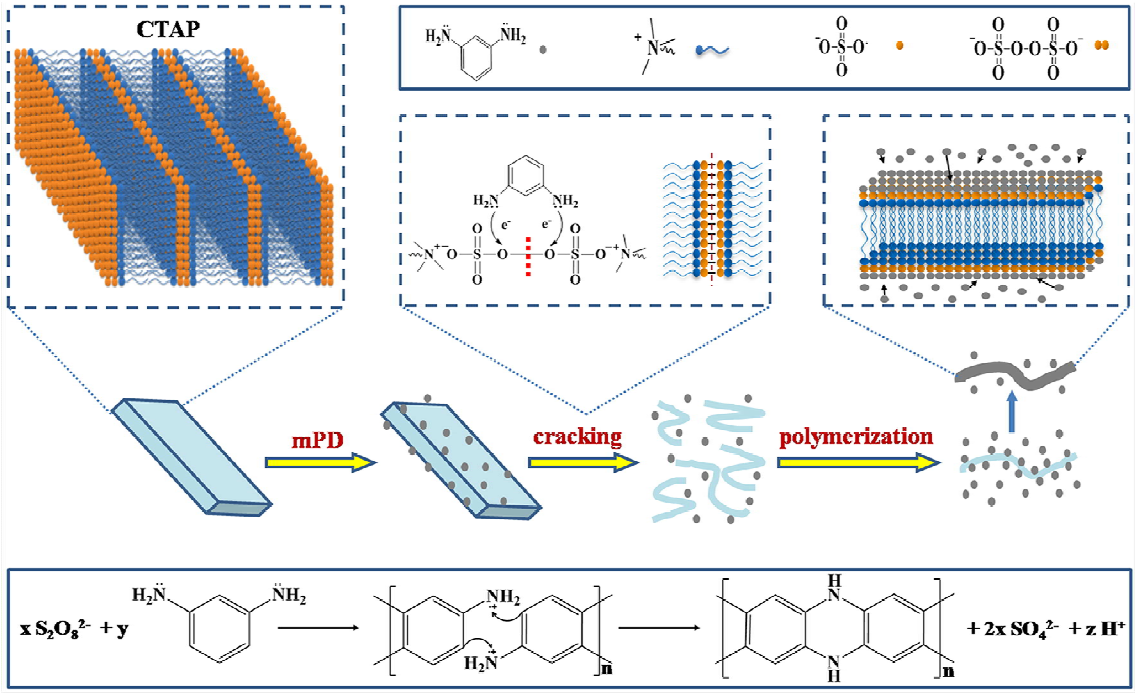

3.2. Discussion on the morphology evolution of PmPD nanobelts

The configuration of CTAP was highly correlated with the oxidative polymerization of m-phenylenediamine and was affected by the CTAB assembly behaviour. In general, CTAB dissolved in water tends to form bilayers due to the amphiphilicity of CTAB molecules. The persulfate anion acts like a link to trigger the parallel piling of these bilayers to constitute the white precipitated powders. Actually, these white precipitates kept the oxidizability of persulfate.[23] So adding m-phenylenediamine into the precipitates suspension initiated the redox reaction. Theoretically, the persulfate decomposed into two sulfate ions and the link for the closely piling of CTAB bilayers is dissociated. The bilayers should gradually release into solution. At the same time to the movement of bilayers, m-phenylenediamine was oxidized into PmPD, which rapidly precipitates onto the bilayers. Finally, the PmPD nanobelts were formed. To verify this opinion, the white precipitates were separated and dried by lyophilization. The precipitates were directly added into m-phenylenediamine solution. The as-prepared PmPD was found to display clearly the nanobelts structure (Fig. S5, ESI†).

3.3. Characterizations

Molecular structure of poly(m-phenylenediamine) was examined with FTIR technique. As shown in Fig. 3, the two peaks between 3000-3600 cm^{-1} are related to the stretching vibration of N-H modes.[24,25] The adsorptions at ~1620 and ~1500 cm^{-1} can be attributed to the stretching vibration of quinoid and benzenoid structures, respectively.[26] The peak at ~1250 cm^{-1} is the vibration of C-N bond.[27] The other three sharp peaks at ~1350, ~1200 and ~1150 cm^{-1} should be linked to the existence of CTAB. It should be noted that the peak at ~1044 cm^{-1} is an indicator of sulfonation of poly(m-phenylenediamine) [13] nearly disappears in these four samples, which suggests the potential function of CTAB to reduce the extent of such side reaction. Anyway, the abundant N-H groups and C-N structure are promising for adsorption application.

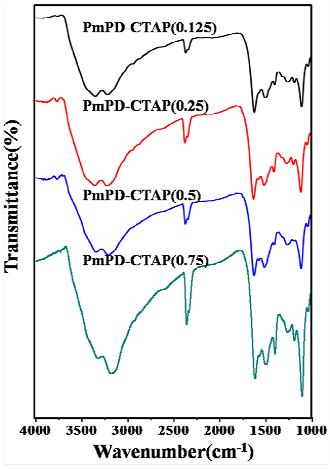

Fig.3 FTIR spectra of poly(m-phenylenediamine).

The supermolecular structure of poly(m-phenylenediamine) was investigated with XRD patterns.[10] In Fig. 4, the four polymers display a common diffraction pattern that only one broad peak at ~25° is found. This means the as-synthesized product is amorphous. Actually, that is beneficial for the adsorption applications since the ions or molecules can relatively readily penetrate into the inner supermolecular structures.[16]

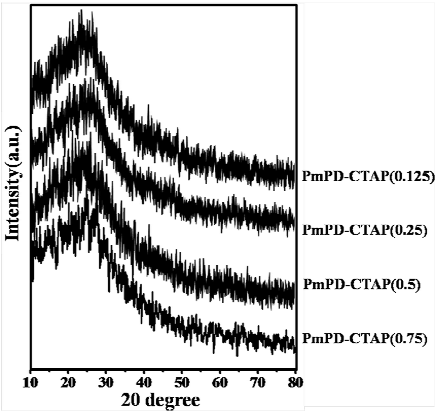

Fig.4 XRD patterns of poly(m-phenylenediamine).

Thermal stability of poly(m-phenylenediamine) nanobelts is a very important factor and TGA-DTA technique was used. As shown in Fig. 5A, the first weight loss of the polymer was found at temperature range of 30-150 °C, and an obvious endothermic peak exists at this temperature range. It can be generally ascribed to the evaporation of water.[15] With further increasing the temperature, the weight of poly(m-phenylenediamine) steadily loses, which should be caused by the complicated degradation of polymeric chains. According to the DTA variation, this reaction is endothermic. Anyway, the thermal stability of poly(m-phenylenediamine) nanobelts is really good and more than 40 % of weight is still remained as the temperature increases to 900 °C. This high char yield also indicates that the poly(m-phenylenediamine) is possibly an ideal feedstock to prepare the carbon materials, which is our future aim.

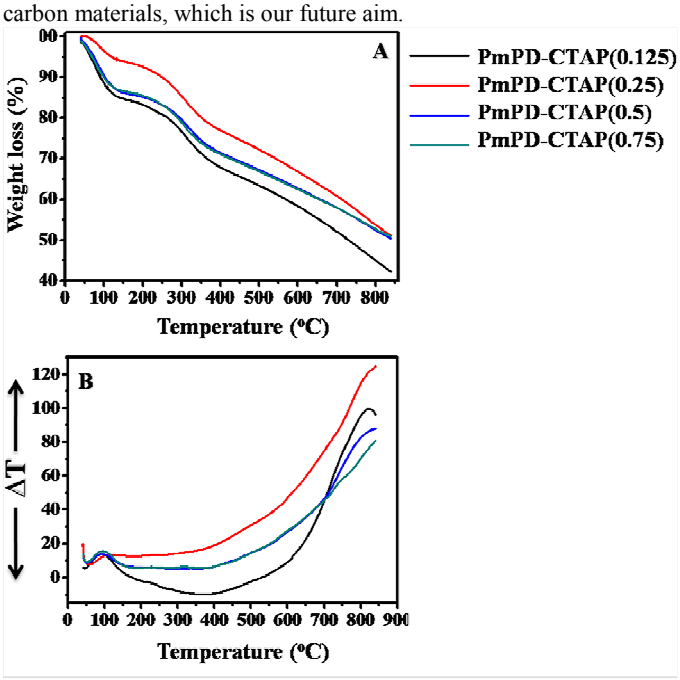

Fig.5 TG (A) and DTA (B) of poly(m-phenylenediamine).

The specific surface area of the PmPD nanobelts was revealed in Table 1. The specific surface area of PmPD-CTAP(0.125) and PmPD-CTAP(0.25) are similar. When the concentration of CTAP increases to 0.5 and 0.75, the specific surface area are 185.498 and 284.545 $m^2 g^{-1}$, respectively. Obviously, the adding of CTAP leads to the increasing of specific surface area of PmPD, and this is beneficial to the adsorption application.

Table 1. The specific surface area and solubility of the PmPD prepared with different CTAP : mPD molar ratio.

PmPD-name	Surface area ($m^2 g^{-1}$)	Solubility[a]					
		NMP	DMSO	DMF	THF	EtOH	H_2O
0.125	40.931	SS	SS	SS	IS	IS	IS
0.25	39.816	SS	SS	SS	IS	IS	IS
0.5	185.498	SS	PS	PS	IS	IS	IS
0.75	284.545	SS	PS	PS	IS	IS	IS

[a] IS represents that the sample is not soluble in a specific solvent, SS represents microscale soluble, PS means partly soluble, and TS signify completely soluble

The solubility of PmPD was also investigated[24], and the data was shown in Table 1. Six solvents were examined, and the products were not soluble in H_2O, THF and EtOH, microscale and partly soluble in NMP, DMSO, DMF. It illustrates that the PmPD products can be used as adsorbent in aqueous solution.

3.4. Adsorption of dyes

Dye pollution has aroused world-wide attention in recent years. In present research, orange G was taken as a prototype to examine the potential of poly(m-phenylenediamine) nanobelts to purify the contaminated water.

3.4.1 Isotherm

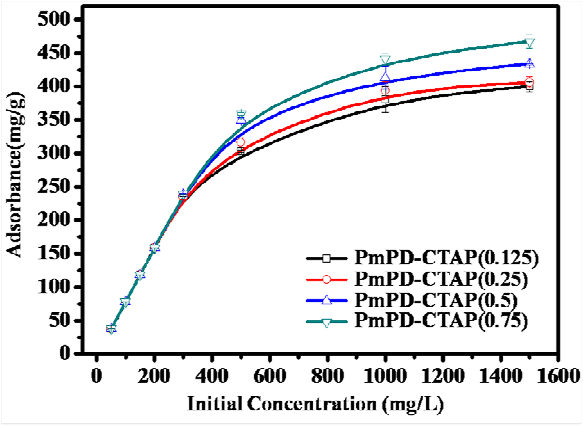

Fig.6 Influence of dye concentration on the adsorption performance of poly(m-phenylenediamine) nanobelts.

The effects of initial Orange G concentration on the adsorption are given in Fig. 6. As seen, the orange G adsorption performance of all adsorbents are almost the same from 0 to 300 mg L^{-1}, but the adsorption curves appear differently with the further enhancement of dye concentration. To give a deeper analysis on the isotherm adsorption, two classical models - Langmuir and Freundlich - were adopted to discuss the adsorption behavior. As shown in Table. S1, ESI†, the fitting coefficient of the adsorption date by Langmuir is much higher than that by Freundlich, which strongly demonstrates the Langmuir model can better describe the adsorption process of orange G by poly(m-phenylenediamine). Actually, the Langmuir model was established based on the hypothesis that the adsorption is saturated after the monolayer of adsorbate on the surface of adsorbent was formed, indicating that the orange G adsorption by poly(m-phenylenediamine) nanobelts is monolayer adsorption. On the other hand, the theoretical maximum adsorbance can be calculated from Langmuir model. The capacity reached 401.61 mg g^{-1} for PmPD-CTAP(0.125), 413.22 mg g^{-1} for PmPD-CTAP(0.25), 434.78 mg g^{-1} for PmPD-CTAP(0.5) and 469.48 mg g^{-1} for PmPD-CTAP(0.75).

In order to interpret the adsorption process and mechanism, we have discussed the characteristic of dye. Dye ion has a tendency to self-associate in aqueous solutions, and the large size of dye molecule can readily trigger aggregation through π-π interactions with each other and with the conjugated materials[28-29]. Influenced by their extensive conjugation, dye aggregates could hardly diffuse into the inner pores of the adsorbent. After the dye adsorption on the outer surface area of conjugated materials, the molecule transport route was blocked, which limited the dye adsorption in the inner surface area. so the dye adsorption by conjugated materials (e.g., carbonaceous materials, conjugated polymers) is highly dependent on their outer surface area (the specific surface area of materials is composed of outer and inner surface area).

Therefore, the adsorption between Orange G and poly(m-phenylenediamine) nanobelts is most probably decided by the π-π conjugate adsorption, and the adsorbing capacity depends on the outer surface area.

Moreover, the adsorption performance of other common materials was illustrated in Table 2. It can be found that most of these materials possess an adsorbance less than 300 mg g^{-1}. Our most recent reported adsorbance by poly(m-phenylenediamine) nanoparticles can reach 370 mg g^{-1}. But it is still less than the performance of poly(m-phenylenediamine) nanobelts, which strongly indicates the superior adsorption ability of poly(m-phenylenediamine) nanobelts toward dye adsorption, especially the orange G.

Table 2. The comparison of Orange G adsorbance of common adsorbents with the PmPD synthesized in this research.

Materials	Adsorbance (mg g^{-1})	References
Magnetic silica	65.89	[30]
Activated carbon	9.129	[31]
Bagasse fly ash	18.796	[32]
Polyaniline	220	[21]
PmPD-CTAP(0.125)	401.61	Current study
PmPD-CTAP(0.25)	413.22	Current study
PmPD-CTAP(0.5)	434.78	Current study
PmPD-CTAP(0.75)	469.48	Current study

3.4.2 Kinetics

Fig. 7 shows the dye concentration in solution at a specific reaction time in the presence of poly(m-phenylenediamine) nanobelts. At the first 200 min, the dye concentration drops rapidly while after that its variation becomes sluggish.

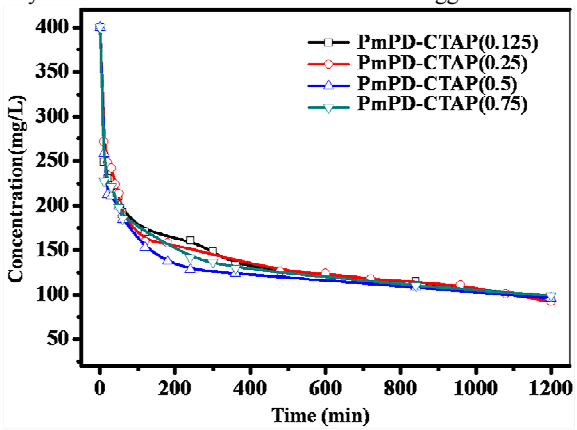

Fig.7 Influence of reaction time on the adsorption performance of poly(m-phenylenediamine) nanobelts.

Pseudo-first-order and pseudo-second-order equations were applied to analyze the data (Table.S2, ESI†). As shown, the pseudo-second-order equation is suitable to fit the adsorption process since its fitting coefficiency is obviously higher than that of the pseudo-first-order equation. That is to say, the interaction between orange G and poly(m-phenylenediamine) nanobelts is chemosorption.[33] Moreover, as the waste water treatment material, the adsorption speed of poly(m-phenylenediamine) nanobelts is very slow and needs to be improved.

3.4.3 The effect of acid doping on the adsorptive property

We have attempted to improve the adsorption rate of PmPD-CTAP(x) by acid doping. The adsorption kinetics and isotherm of acid doping poly(m-phenylenediamine) samples are studied.

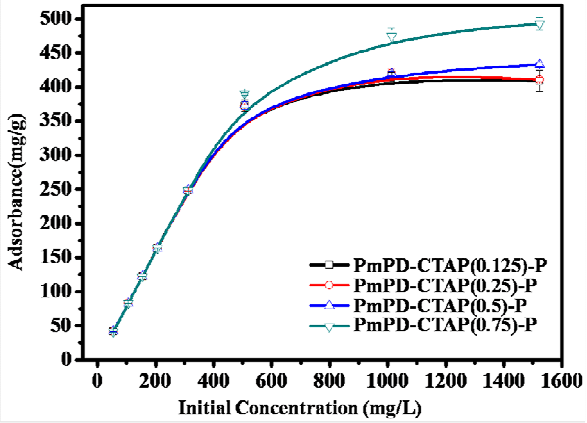

Fig.8 Influence of dye concentration on the adsorption performance of acid doping poly(m-phenylenediamine) nanobelts.

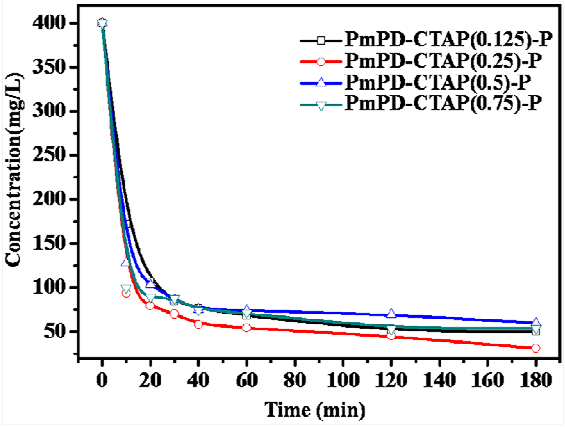

Fig.9 Influence of reaction time on the adsorption performance of acid doping poly(m-phenylenediamine) nanobelts.

From the Fig.8, the adsorbents reached saturation when the concentration is more than 1000 mg L^{-1}. To describe the adsorption behaviour, Langmuir and Freundlich models were adopted. The fitting coefficient of the adsorption date by Langmuir can better describe the adsorption since the correlation efficiency of >0.99 is much higher than that of Freundlich. Through the calculation with Langmuir model, the Orange G adsorption capacity of the PmPD was obtained (Table S4†). The capacity reached 413.22 mg g^{-1} for PmPD-CTAP(0.125)-P, 416.67 mg g^{-1} for PmPD-CTAP(0.25)-P, 434.78 mg g^{-1} for PmPD-CTAP(0.5)-P and 497.51 mg g^{-1} for PmPD-CTAP(0.75)-P. The acid doping makes the PmPD-CTAP(x)-P positively charged and shows electropositive, and the Orange G is in the form of the anion. Therefore, the adsorption mechanism most probably is the electrostatic adsorption and original π–π complex adsorption have been destroyed.

Comparing Fig.7 and Fig.9, it is found that the required time to attain equilibrium adsorption has been shortened from 600 minute to 60 minute. Pseudo-first-order and pseudo-second-order equations were also applied to analyze the data (Table.S5, ESI†). As shown, the pseudo-second-order-equation is suitable to fit the adsorption process and the interaction between orange G and PmPD-CTAP(x)-P is chemosorption[34].

Conclusions

PmPD nanobelts have been successfully synthesized by chemically oxidative polymerization using CTAP as oxidant. The PmPD nanobelts possessed high surface area of 284.5 m^2 g^{-1}, low solubility in common solvents and good thermal stability. Moreover, the PmPD nanobelts showed superior ability towards Orange G adsorption with a maximum adsorbance of 460 mg g^{-1}. The adsorption behavior can be described by pseudo-second-order and Langmuir models. The acid doping of PmPD nanobelts could generate better adsorption performance for Orange G. The PmPD nanobelts can also be applied in the field of biosensors, catalysis and anticorrosion.

Acknowledgement

This research was financially supported by Natural Science Foundation of China (51374237), Chang Jiang Scholars Program (T2011116), Shanghai Tongji Gao Tingyao Environmental Science & Technology Development Foundation and Young Scholarship Award for Doctoral Candidate Issued by Ministry of Education (1343-76140000018).

Notes and references

[a] *Department of Environmental Engineering, School of Metallurgy and Environment, Central South University, Changsha 410017, China. E-mail: haiyw25@yahoo.com; Fax:+86-0731-88710171; Tel: +86-0731-88836804*

[b] *National Engineering Research Central for Heavy Metals Pollution Control and Treatment, Changsha 410017, China. E-mail: haiyw25@yahoo.com; Fax:+86-0731-88710171; Tel: +86-0731-88836804*

[c] *Department of Environmental Monitoring, Changsha Environmental Protection College, 410004, China.*

‡ *Yun Meng and Liyuan Zhang contributed equally to this research.*

† Electronic Supplementary Information (ESI) available: [Fig. S1, ESI†: The synthesis sketch map of the PmPD; Fig. S2, ESI†: The SEM images of precursor (white precipitates); Fig. S3, ESI†: TEM images of PmPD synthesized with the organic solvents (Methanol); Fig. S4, ESI†: TEM images of PmPD prepared in aqueous medium with traditional oxidation polymerization; Fig. S5, ESI†: The morphology evolution from CTAB bilayers to PmPD nanobelts; Fig. S6, ESI†: N_2 adsorption-desorption isotherm of poly(m-phenylenediamine); Fig.S7, ESI†: Selectivity adsorption of the acid doping poly(m-phenylenediamine) towards different types of dye; Fig.S8 , ESI†: SEM images of PmPD synthesized with the different reaction time; Fig.S9, ESI†: SEM images of PmPD synthesized with the different stirring rate. Table. S1, ESI†: Isotherm model equations for Orange G adsorption onto the poly(m-phenylenediamine); Table. S2, ESI†: Kinetics model equation for Orange G adsorption onto the PmPD; Table. S3, ESI†: the relationship between

adsorbance and surface area of different adsorbtents; Table.S4, ESI†: Isotherm model equations for Orange G adsorption onto the acid doping poly(m-phenylenediamine); Table.S5 , ESI†: Kinetics model equation for Orange G adsorption onto the acid doping poly(m-phenylenediamine)].
See DOI: 10.1039/b000000x/

(1) Li, X. G.; Huang, M. R.; Duan, W.; Yang, Y. L. *Chemical Review,* **2002,** *102*, 2925-3030.
(2) Tian, J. Q.; Li, H. L.; Lu, W. B.; Luo, Y. L.; Wang, L.; Sun, X. P. *Analyst,* **2011,** *136*, 1806-1809.
(3) Tian, J. Q.; Luo, Y. L.; Li, H. L.; Lu, W. B.; Chang, G. H.; Qin, X. Y.; Sun, X. P. *Catalyst Scencei Technology,* **2011,** *1*, 1393-1398.
(4) Zhang, Y. W.; Li, H. L.; Luo, Y. L.; Shi, X.; Tian, J. Q.; Sun, X. P. *Plos One,* **2011,** *6*, 1-10.
(5) Zhang, Y. W.; Wang, L.; Tian, J. Q.; Li, H. L.; Luo, Y. L.; Sun, X. P. *Langmuir,* **2011,** *27*, 2170-2175.
(6) Chai, L.-Y.; Yu, W.-T.; Wang, H.-Y.; Zhang, L.-Y. *Micro & Nano Letters,* **2012,** *7* (12), 1264-1266.
(7) Tang, R.; Li, Q.; Ding, L.; Cui, H.; Zhai, J. *Environmental Technology,* **2012,** *33* (3), 341-348.
(8) Huang, M. R.; Lu, H. J.; Li, X. G. *J. Colloid Interface Science,* **2007,** *313* (1), 72-79.
(9) Huang, M.-R.; Lu, H.-J.; Song, W.-D.; Li, X.-G. *Soft Materials,* **2010,** *8* (2), 149-163.
(10) Huang, M.-R.; Peng, Q.-Y.; Li, X.-G. *Chemistry-A European Journal,* **2006,** *12* (16), 4341-4350.
(11) Lu, Q. F.; Huang, M. R.; Li, X. G. *Chemical European, J.* **2007,** *13* (21), 6009-6018.
(12) Su, Z.; Zhang, L.; Chai, L.; Wang, H.; Yu, W.; Wang, T.; Yang, J. *New Journal of Chemistry,* **2014**.
(13) Su, Z.; Zhang, L.; Chai, L.; Yu, W.; Wang, H.; Shi, Y. *Rsc Advances,* **2013,** *3*, 8660-8665.
(14) Yu, W.; Zhang, L.; Meng, Y.; Dai, S.; Su, Z.; Chai, L.; Wang, H. *Synthetic Metals,* **2013,** *176*, 78-85.
(15) Yu, W.; Zhang, L.; Wang, H.; Chai, L. *Journal of hazardous materials,* **2013,** *260*, 789-95.
(16) Zhang, L.; Chai, L.; Liu, J.; Wang, H.; Yu, W.; Sang, P. *Langmuir ,***2011,** *27*, 13729-38.
(17) Yu, W.; Zhang, L.; Meng, Y.; Dai, S.; Su, Z.; Chai, L.; Wang, H. *Synthetic Metals,***2013,** *176*, 78-85.
(18) Wang, T.; Zhang, L.; Wang, H.; Yang, W.; Fu, Y.; Zhou, W.; Yu, W.; Xiang, K.; Su, Z.; Dai, S. *ACS applied materials & interfaces,* **2013,** *5* (23), 12449-12459.
(19) Pan, Z. W.; Dai, Z. R.; Wang, Z. L. *Science,* **2001,** *291* (5510), 1947-9.
(20) Ayad, M. M.; El-Nasr, A. A. *The Journal of Physical Chemistry C,* **2010,** *114* (34), 14377-14383.
(21) Mahanta, D.; Madras, G.; Radhakrishnan, S.; Patil, S. *The Journal of Physical Chemistry B,* **2008,** *112* (33), 10153-10157.
(22) Zhang, L.; Wang, H.; Yu, W.; Su, Z.; Chai, L.; Li, J.; Shi, Y. *Journal of Materials Chemistry,* **2012,** *22* (35), 18244.
(23) Chen, T.; Du, B.; Fan, Z. *Langmuir : the ACS journal of surfaces and colloids,* **2012,** *28* (42), 15024-32.
(24) Li, X.-G.; Ma, X.-L.; Sun, J.; Huang, M.-R. *Langmuir,* **2009,** *25* (3), 1675-1684.
(25) Huang, M. R.; Peng, Q. Y.; Li, X. G. *Chemistry-A European Journal,* **2006,** *12* (16), 4341-4350.
(26) Wang, J. J.; Jiang, J.; Hu, B.; Yu, S. H. *Advanced Functional Materials,* **2008,** *18* (7), 1105-1111.
(27) Chai, L.; Zhang, L.; Wang, H.; Yu, W.; Sang, P. *Materials Letters,* **2010,** *64* (21), 2302-2305.
(28) Walker, G. M.; , L. R. W. *Chemical Engineering Journal,* **2001,** *83*, 201–206.
(29) Chien-To Hsieh, H. T. *Carbon,* **2000,** *38* 863–869.
(30) Atia, A. A.; Donia, A. M.; Al-Amrani, W. A. *Chemical Engineering Journal,* **2009,** *150* (1), 55-62.
(31) Arulkumar, M.; Sathishkumar, P.; Palvannan, T. *Journal of hazardous materials,* **2011,** *186* (1), 827-834.
(32) Mall, I. D.; Srivastava, V. C.; Agarwal, N. K. *Dyes and pigments,* **2006,** *69* (3), 210-223.
(33) Xin-Gui Li; Xiao-Li Ma; Jin Sun; Huang, a. M.-R. *Langmuir,* **2009,** *25*, 1675-1684.
(34) Li, X.-G.; Ma, X.-L.; Sun, J.; Huang, M.-R. *Langmuir,* **2009,** *25*, 1675-1684.